Cerebral Cortex December 2010;20:2939–2947
doi:10.1093/cercor/bhq041
Advance Access publication March 26, 2010

Unilateral Cortical Spreading Depression Affects Sleep Need and Induces Molecular and Electrophysiological Signs of Synaptic Potentiation In Vivo

Ugo Faraguna[1], Aaron Nelson[1,2], Vladyslav V. Vyazovskiy[1], Chiara Cirelli[1] and Giulio Tononi[1]

[1]Department of Psychiatry and [2]Neuroscience Training Program, University of Wisconsin–Madison, Madison, WI 53719, USA

Address correspondence to Giulio Tononi, MD, PhD, Department of Psychiatry, University of Wisconsin–Madison, 6001 Research Park Boulevard, Madison WI 53719, USA. Email: gtononi@wisc.edu.

Cortical spreading depression (CSD) is an electrophysiological phenomenon first described by Leao in 1944 as a suppression of spontaneous electroencephalographic activity, traveling across the cerebral cortex. In vitro studies suggest that CSD may induce synaptic potentiation. One recent study also found that CSD is followed by a non-rapid eye movement (NREM) sleep duration increase, suggesting an increased need for sleep. Recent experiments in animals and humans show that the occurrence of synaptic potentiation increases subsequent sleep need as measured by larger slow wave activity (SWA) during NREM sleep, prompting the question whether CSD can affect NREM SWA. Here, we find that, in freely moving rats, local CSD induction increases corticocortical evoked responses and strongly induces brain derived neurotrophic factor (*BDNF*) in the affected cortical hemisphere but not in the contralateral one, consistent with synaptic potentiation in vivo. Moreover, for several hours after CSD, large slow waves occur in the affected hemisphere during rapid eye movement sleep and quiet waking but disappear during active exploration. Finally, we find that CSD increases NREM sleep duration and SWA, the latter specifically in the affected hemisphere. These effects are consistent with an increase in synaptic strength triggered by CSD, although nonphysiological phenomena associated with CSD may also play a role.

Keywords: cerebral cortex, EEG, rat, slow wave activity

Introduction

Unilateral cortical spreading depression (CSD) is a self-propagating wave of cellular depolarization followed by a marked enduring reduction of spontaneous electrical activity (Leao 1944; Smith et al. 2006). CSD is a transient phenomenon, can be experimentally localized to the cortical hemisphere where it is induced, and has been widely used to induce functional decortication (Shibata and Bures 1974; Best et al. 1975; Monda et al. 2000). The mechanisms underlying CSD induction and propagation remain unclear (Lauritzen 1994). It is known, however, that during CSD, both neurons and glial cells depolarize (Sugaya et al. 1975), and it is likely that the broad syncytium made up of astrocytes and their gap junctions contributes to the CSD depolarization spread (Walz 2000; Kitahara et al. 2001).

Two in vitro studies suggest that CSD may be capable of locally inducing cortical synaptic potentiation (Footitt and Newberry 1998; Berger et al. 2008). Specifically, one study that used human neocortical slices collected during surgery for intractable epilepsy found that CSD significantly enhanced the amplitude of excitatory postsynaptic potentials and increased the induction of long-term potentiation (LTP) in cortical layer III (Berger et al. 2008). Another study that used an in vitro model of CSD found that KCl application to the rat neocortex was followed by a sustained LTP-like enhancement of synaptic transmission (Footitt and Newberry 1998). However, whether CSD can induce similar effects in vivo remains untested. Moreover, whether these changes reflect physiological phenomena is also unclear because CSD is associated with energy depletion and cell swelling (Krivanek 1976; Csiba et al. 1985; Lauritzen et al. 1990; Takano et al. 2007; Hashemi et al. 2009), although not with irreversible brain damage (Nedergaard and Hansen 1988).

The effects of CSD on sleep are also poorly understood. One recent study in rats found that CSD increases non-rapid eye movement (NREM) sleep duration, suggesting an increased need for sleep (Cui et al. 2008). However, that study did not assess whether electroencephalographic (EEG) activity during waking was also affected nor did it test whether sleep intensity may have increased more in the cortical hemisphere that underwent CSD relative to the contralateral one. This may be revealing because there is increasing experimental evidence suggesting that sleep slow waves can be regulated at a local level based on prior waking activity (Krueger et al. 1995, 2008; Tononi and Cirelli 2003, 2006).

Specifically, recent studies show that the occurrence of synaptic potentiation in specific neural circuits increases subsequent sleep need in those circuits, suggesting a link between synaptic potentiation and sleep homeostatic regulation (Tononi and Cirelli 2003, 2006). Sleep intensity and sleep need are accurately indexed by an established electrophysiological marker, called slow wave activity (SWA), which is defined as the EEG power spectrum in the 0.5–4.0 Hz frequency range during NREM sleep. SWA increases as a function of waking duration, decreases during sleep, is further increased by sleep deprivation, and is reduced by naps (Achermann and Borbely 2003). Moreover, local cortical application of brain derived neurotrophic factor (*BDNF*) produces a localized increase in SWA (Faraguna et al. 2008), consistent with the causal role of *BDNF* in some forms of LTP. More stringently, training on a reaching task known to induce LTP also results in a local increase in SWA in the activated rat motor region (Hanlon et al. 2009). Thus, in this study, we induced CSD in freely moving rats by local infusion of KCl on top of the occipital cortex to test whether the induction of CSD leads to the occurrence of cortical synaptic potentiation in vivo. If so, we hypothesized that a unilateral increase in synaptic strength triggered by CSD should be followed by a unilateral change in sleep intensity as measured by SWA.

Materials and Methods

Surgery

Male Wistar Kyoto rats (250–300 g at time of surgery; 10- to 15-week-old; Charles River Laboratories) were maintained on a 12-h light/dark

cycle (lights on at 10:00 AM; room temperature, 23 ± 1 °C). Under deep isoflurane anesthesia (1.5–2% volume), rats were implanted for chronic EEG recordings with bipolar concentric local field potential (LFP) electrodes (interelectrode distance 0.75 mm for parietal and 1.25 mm for frontal derivations; Rhodes Medical Instruments) bilaterally in frontal cortex (from bregma: anteroposterior [AP] +2 mm, mediolateral [ML] ±3.0 mm) and parietal cortex (from bregma: AP –2.5 mm, ML ±4–5 mm), along with one reference epidural screw over the cerebellum and another cerebellar screw as ground. Electrodes were connected to stainless steel wires soldered to a plug and fixed to the skull with dental cement. Two stainless steel wires (diameter 0.4 mm) inserted into the neck muscles served to record the electromyogram (EMG). A cannula (part number: C315GA/SPC; Plastics1) for the delivery of KCl or NaCl was placed unilaterally over the occipital cortex (AP –8.0 mm and ML +3.0 mm) so that the cannula's tip barely protruded (~0.1 mm) through the burr hole. The cannula was kept patent by inserting a removable obturator. Immediately after surgery, the animals were individually placed in transparent Plexiglas cages (36.5 × 25 × 46 cm) and kept in sound-attenuating recording boxes for the duration of the experiment. At least 1 week was allowed for recovery after surgery, and experiments were started only after the sleep/waking cycle had normalized. The rats were connected by means of a flexible cable to a commutator (Airflyte) and recorded continuously. Every day beginning the day after surgery, rats were handled between 10:00 AM and 10:30 AM to habituate them to the injection procedure (see below). Video recordings were performed continuously with infrared cameras (OptiView Technologies) and stored in real time (AVerMedia Technologies). To verify that the animals were fully entrained to the light/dark cycle, all cages were equipped with Chronokit activity monitor infrared sensors (Stanford Chronokit; Stanford Software Systems). All animal procedures followed the National Institutes of Health *Guide for the Care and Use of Laboratory Animals*, and facilities were reviewed and approved by the Institutional Animal Care and Use Committee of the University of Wisconsin–Madison and were inspected and accredited by the Association for the Assessment and Accreditation of Laboratory Animal Care.

Data Acquisition

Rats were connected by means of a flexible cable and a commutator to a Grass mod. 8 polygraph (Grass Instruments). LFP and EMG signals were conditioned by analog filters (high pass, 0.1 Hz; low pass, 35 Hz), digitalized at 128 Hz (Kissei America), and stored in a computer. Waking, NREM, and rapid eye movement (REM) sleep states were visually determined in 4-s epochs based on the LFP, electrocorticogram (obtained by referencing the superficial lead of the LFP electrode to a "neutral" cerebellar screw), and EMG recordings according to standard criteria. Visual scoring was manually performed off-line (Sleep Sign; Kissei COMTEC). Artifacts were always removed simultaneously from all derivations and vigilance states could always be determined. LFP power spectra (fast Fourier transform routine, Hanning window) were calculated for consecutive 4-s epochs within the 0.25–20.0 Hz frequency range. Vigilance states were scored by the same scorer twice, separately for the 2 hemispheres. A 4-s epoch was defined as "dissociated" if the scoring for left and right hemispheres was discordant (wake on one side and NREM sleep on the other side).

Injection Procedure

Rats were habituated to the injection procedure by daily handling. On the injection day, the procedure included several steps: removal of the obturator, insertion of the injector, and delivery of the compound. Total volume and infusion rate were optimized in pilot experiments to induce unilateral CSD. All solutions were infused through polyethylene tubing connected to a Hamilton syringe controlled by a microinfusion pump (CMA 400 Syringe Pump; CMA Microdialysis). The injector was removed 5–10 min after the end of the injection to avoid backflows and immediately replaced with the obturator. In each animal, only one side was injected (same side throughout the entire experiment). The delivery rate was modified in real time for the different CSD duration groups (see below).

Experimental Design

To consistently induce CSD, KCl was infused over the occipital cortex. All infusions were performed in freely moving unrestrained animals, at least 1 week after surgery. During the induction of CSD and afterward, rats were always left undisturbed in their recording cage. In all groups, KCl (diluted in sterile pyrogen-free water) was injected first, soon after lights on (between 10:40 AM and 11:15 AM) in either the left or the right hemisphere in a balanced manner within groups. Rats were assigned to 5 different experimental groups: 3 groups for electrophysiological experiments (1-h CSD, $n = 6$ rats; 5-min CSD, $n = 6$; 1-h CSD for evoked responses [ERs], $n = 8$) and 2 groups for molecular studies (1-h CSD, $n = 4$ rats; 5-min CSD, $n = 7$). With the exception of 2 rats in the first group (1-h CSD) that received KCl 3 M, all animals were injected with KCl 1.5 M because the latter allowed a better control of the duration of CSD. Since CSD can persist for several minutes after the end of the infusion, the delivery of KCl was stopped after 3 and 45 min to induce CSD of approximately 5 and 60 min, respectively. In the first group of animal (1-h CSD, $n = 6$), a second injection of NaCl (1.5 M; 3 M in the 2 rats injected with KCl 3 M) occurred at least 4 days after the induction of CSD, matching the timing and duration of the KCl infusion. CSD duration (mean ± standard error of mean [SEM], in minutes) was as follows: 55.2 ± 7.8 (group 1), 5.2 ± 1.2 (group 2), 58.8 ± 3.2 (group 3), 66.4 ± 5.2 (group 4), and 5.5 ± 2.2 (group 5). All groups were implanted with parietal LFP and EMG electrodes, while frontal electrodes were implanted in the animals used for the ER recordings ($n = 8$). In a subset of animals belonging to group 1 ($n = 4$), both frontal and parietal LFP signals were recorded.

Real-Time Quantitative PCR

Real-time quantitative PCR (qPCR) was performed as described (Cirelli et al. 2004). Briefly, reverse transcription reactions were carried out in parallel on DNase I digested pooled total RNA from left and right cortices. Prior to reverse transcription, total RNA was confirmed to be free of contaminating DNA sequences by PCR using rat β-actin-specific primer pairs designed to differentiate between complementary DNA, genomic DNA, and pseudogene genomic DNA. Eight reverse transcription reactions were performed for each sample. Reverse transcription reactions were as follows: 100 ng total RNA, 2.5 μL oligo dT_{16} (500 μg/mL), 5 μL dNTPmix (10 mM each dNTP), 1 pg artificial transcript (IDT, Inc.), and H_2O to 29.75 μL. Samples were incubated at 70 °C for 10 min, put briefly on ice, and then incubated at 42 °C for 2–5 min. Mix #2 (10 μL 5× Superscript II First Strand Buffer, 5 μL 0.1 M dithiothreitol, 4 μL 25 mM $MgCl_2$, and 1.25 μL Superscript II RNase H^- Reverse Transcriptase 200 U/μL) was added and mixed, and samples were immediately returned to incubate at 42 °C for 1 h. Reactions were stopped by incubation at 70 °C for 15 min. PCRs to measure levels of artificial transcript were done to confirm uniformity of reverse transcription within sample groups and between samples. Each PCR contained specific forward and reverse primers (200–750 nM final concentration), 2× SYBR Green Master Mix (used at 3.2×), 5 μL of a 1:10 dilution of pooled reverse transcription product, and H_2O to a total volume of 25 μL. A 2-step PCR profile was used: 10 min at 95 °C denaturation and Amplitaq gold activation, followed by 40 cycles alternating between 95 °C for 15 s and 60 °C for 60 s. PCR was done in quintuplicate for each sample condition assayed and relative quantities determined based on the equation of the line of best fit derived from the standard curve ($R^2 \geq 0.985$). The following primers were used: *Arc*: forward, TGCACATAAACCATGACCCATACT; reverse, TGGATATT-GAAGGCTTGGTGAA; *BDNF*: forward, GCAAGGGCCAGGTCGATTA; reverse, GGTATGAGAGCCAGCCACTGA; and *NGFI-A*: forward, TTTGCCCGTCCCTTTGGT; reverse, CGGCAAGGTGTGTCACACA. For statistical analysis, the arbitrary values obtained for each hemisphere were expressed as percentage relative to the mean value between the 2 hemispheres.

Evoked Responses

Transcallosal corticocortical ERs were recorded as described (Vyazovskiy et al. 2008). An S-88 Dual Output Square Pulse Stimulator and a stimulus isolating unit (PSIU-6; Grass-Telefactor, AstroMed, Inc.) were used for electrical stimulation, which consisted of single

monophasic squared pulse, 0.1 ms in duration. Each recording session lasted approximately 1–5 min, during which a sufficient number of artifact-free responses were collected (on average ~40, at irregular intervals ranging from 3 to 10 s). Responses were recorded from the frontal cortex (M1, B: +2–3 mm, L: 2–3 mm) after electrical stimulation of the contralateral homotopic area. After each session, all individual responses were visually screened by an experimenter blind to their origin, and only those that were recorded on a background of stable low-amplitude high-frequency cortical activity were used for further analysis. ERs show substantial and predictable changes in shape and/or amplitude with changes in behavioral state, and in some individuals, a few responses (less than 5%) were discarded on that basis (largely due to brief movements immediately before the investigator triggered the stimulation). ERs were recorded with 5-kHz sampling rate (analog filters: high-pass filter: attenuation 50% amplitude at 0.1 Hz; low-pass filter: attenuation 50% amplitude at 1 kHz). ERs were collected during quiet waking. To standardize this behavioral state as much as possible, behavior and EEG and EMG activity of each rat were monitored for the entire stimulation session and for the preceding 10 min, during which the investigator kept each cage open and made sure the animals were not asleep (rats had been habituated to this protocol for at least 1 week). Arousal was induced by acoustic stimuli while direct contact with the animals was always avoided. Stimuli were delivered manually only when the rat was quietly awake (immobile, eyes open, low EMG tone, and low-voltage high-frequency cortical EEG activity). Prior to the experiment, input–output tests were performed in each rat. First, stimulus intensity was varied in the range between 0.1 and 7 mA (in most cases <2 mA) to obtain a clearly identifiable early ER component. For the experiment 1, intensity was selected, corresponding to approximately 50% of the intensity necessary to induce a motor response. The early component of the ER consisted of a depth-negative wave with a latency to the peak of approximately 4–5 ms.

Histological Verification

Upon completion of the experiments, the position of the LFP electrodes was verified by histology in all animals. Perfusion was performed under deep isoflurane anesthesia (3% in oxygen), with saline followed by a 4% solution of paraformaldehyde (PFA) in 0.1 M sodium phosphate, pH 7.2. Brains were postfixed overnight in 4% PFA, cryoprotected in increasing concentration of sucrose (15%, 20%, and 30%) in phosphate-buffered saline, rapidly frozen on dry ice, cut into 50-μm serial coronal sections, and subjected to cresyl violet (Nissl) staining. In all cases, the deep LFP electrode was located within layer V, whereas the superficial LFP electrode was in layers I–II.

Statistical Analysis

Statistical analysis was performed with Statistica (StatSoft). Statistical significance ($^*P < 0.01$ if not specified otherwise) was tested either with Bonferroni correction after 2-way analysis of variance (ANOVA) for SWA (factors: time and hemisphere) and sleep duration (factors: time and treatment) time course or with paired *t*-test for the bin-wise comparison of relative EEG spectra and qPCR measures. For ER experiments, significance was tested with Newman–Keuls test after significance in ANOVA. Data processing was done with custom-made scripts in Matlab (MathWorks, Inc.).

Results

CSD Includes 2 Distinct Phases

After an undisturbed 24-h baseline, rats ($n = 6$) were injected with KCl soon after lights on to induce CSD for approximately 1 h (Fig. 1*A*,*B*). Within a few minutes after the onset of KCl delivery in the occipital cortex, the LFP signal recorded from the parietal derivation ipsilateral to the infusion showed a flattening of the EEG signal (Fig. 1*C*), while the contralateral hemisphere did not show any abnormal EEG sign. As shown in the example of Figure 1*C*, the traveling wave of CSD was evident first in the parietal derivation and later (with an ~15-s delay) in the frontal derivation. During the approximately 1 h of CSD (55.2 ± 7.8 min), rats were asleep approximately 50% of the time, and the behavioral state of all animals was always consistent with the electrical activity of the contralateral hemisphere. Sleep duration did not differ from the control (1 h of CSD, percentage of time spent asleep according to the noninjected hemisphere: 50.1 ± 3.1 after KCl vs. 49.2 ± 4.7 after NaCl, ns, $P = 0.92$). During waking, the animals were ataxic but did not seem to be in pain. Two rats tried to grasp a food pellet while CSD was occurring but appeared unable to control the paw contralateral to the affected hemisphere. Between each cycle of CSD with isoelectric EEG, a phase characterized by high-amplitude negative spikes was detected (Fig. 1*D*). This phase most likely reflects the occurrence of brief bursts of intense single-unit activity, as previously described (Grafstein 1956; Morlock et al. 1964; Sugaya et al. 1975). As soon as both phases were no longer detectable, CSD was considered terminated, and the following period was defined as recovery.

Dissociation of Behavioral States during Recovery from CSD

Behavioral states were always scored based on the EEG activity in the noninjected hemisphere. However, analysis of the raw EEG traces revealed an interesting dissociation in the electrical activity of left and right cortices. Specifically, as soon as CSD ended, slow waves visually indistinguishable from those normally observed during NREM sleep started appearing in the CSD hemisphere, while the contralateral one showed signs of either waking or REM sleep (Fig. 2*A*–*C*). During this dissociated state, the behavior was always consistent with the EEG of the noninjected hemisphere: both eyes were open, and the rats were immobile or grooming or slowly moving around while slow waves could be seen in the hemisphere that previously underwent CSD. However, these waves disappeared when the rats were engaged in active exploration. In other words, there were never signs of dissociation during active exploration with intense movements. During the first hour of recovery, slow waves occurred in approximately 40% of all periods of waking and REM sleep (Fig. 2*D*), but 12 h later, this dissociation had disappeared in all animals. Analysis of the EEG power spectrum in the 0.5–20 Hz range confirmed that the changes in REM and waking were confined to the lower frequencies encompassing SWA (<6 Hz), were largest during the first 4-h interval from sleep onset, and had largely disappeared 10 h after sleep onset (Fig. 2*E*).

CSD Results in an Early Increase in NREM Sleep Duration at the Expense of REM Sleep

During early recovery after CSD, the duration of NREM sleep increased as compared with the corresponding NaCl control (249 ± 9 vs. 225 ± 5 min across the first 6 h starting from CSD termination; $P = 0.05$; $n = 6$; Fig. 3*A*). This increase occurred mainly at the expense of REM sleep (126 ± 2 vs. 88 ± 9 min over the light period; $P < 0.01$) (Fig. 3*A*). The increase in NREM sleep duration was followed by a significant decrease during the early part of the dark phase (210 ± 9 vs. 187 ± 5 min across the entire dark period; $P < 0.01$), so that the total duration of NREM sleep during the 24 h after CSD did not change (578.9 ± 10.1 vs. 591.5 ± 13.0 min; $P = 0.47$).

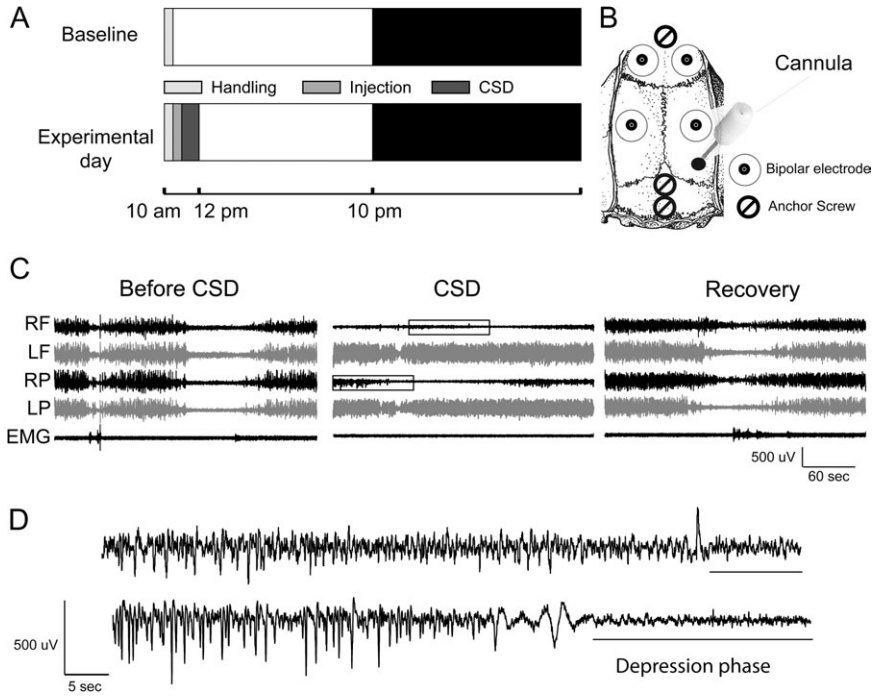

Figure 1. (*A*) Experimental design. Each day after surgery, rats were gently handled for a few minutes after light onset. After an undisturbed 24-h baseline, rats were injected soon after lights on with KCl or, at least 4 days later, with NaCl. (*B*) Implant layout with LFP electrodes in frontal and parietal cortices, anchor screws over frontal cortex and cerebellum, and the injection cannula over the occipital cortex. (*C*) Raw LFP recordings. Examples of LFP recordings (from top to bottom, right frontal [RF], left frontal [LF], right parietal [RP], and left parietal [LP]) and corresponding EMG are shown during baseline (left panel), during a cycle of CSD (middle panel), and during recovery (after all signs of CSD have disappeared). (*D*) The 2 phases (negative spikes and depolarization) of CSD are magnified from the boxed inserts in (*C*), middle panel.

CSD Unilaterally Increases Sleep SWA

SWA at sleep onset is significantly affected by sleep/wake history (Tobler 2005). A significant advantage for SWA analysis in this study was therefore that CSD was confined to one side of the cortex, while both affected and nonaffected hemispheres shared the same sleep/wake history up to the time of CSD induction. For the first two 2-h intervals during recovery after CSD, SWA was increased on the affected side compared with the contralateral one (SWA as percentage of baseline, first 2 h: 162.9 ± 6.2 vs. 140.6 ± 3.6; second 2 h: 156.2 ± 9.7 vs. 134.7 ± 5.0; $P < 0.01$; $n = 6$; Fig. 3*B*). This increase was specific for the lower frequencies of the EEG spectrum (<3.75 Hz) and occurred at the expense of the faster frequencies (Fig. 3*C*). In a different group of rats where CSD was induced for a shorter amount of time (5.2 ± 1.2 min; $n = 6$), SWA showed a smaller increase, and the effect lasted only for the first 2 h of recovery (Fig. 3*D*,*E*), suggesting that the SWA increase in the hemisphere that underwent CSD was "dose dependent." SWA in the contralateral hemisphere did not differ after KCl injection (CSD induction) relative to NaCl injection (control; Supplementary Fig. 1). Thus, CSD has a global effect on NREM sleep quantity, resulting in an early increase in its duration but not on NREM sleep quality since SWA changes were restricted to the affected hemisphere.

During the approximately 1 h of CSD, rats were asleep for approximately half of the time, as indicated by their behavior and the EEG activity in the nonaffected hemisphere. The cortex undergoing CSD, on the other hand, showed long periods of isoelectric EEG alternating with short periods with high-amplitude negative spikes, both of which differ significantly from the neuronal activity observed during physiological NREM sleep. An unlikely possibility, therefore, is that the unilateral increase in SWA in the affected hemisphere had resulted from the unilateral "sleep deprivation" that occurred during CSD. However, previous experiments have shown that SWA shows only negligible changes after 1 h of sleep deprivation, suggesting that sleep loss per se, namely the lack of slow waves, is unlikely to account for the large increase in SWA observed after CSD. Moreover, in the single rat that remained awake for the entire duration (~1 h) of CSD, we still found that SWA was significantly larger in the affected hemisphere relative to the contralateral one (Supplementary Fig. 2).

CSD Induced a Unilateral Increase in Slope and Amplitude of Corticocortical ERs

In another set of animals ($n = 8$), transcallosal corticocortical ERs were recorded within 30 min from light onset before CSD, as soon as approximately 1-h CSD had ended, and after approximately 4 h of recovery after CSD (Fig. 4*A*,*B*). Responses were evoked in the nonaffected frontal cortex and recorded in the frontal cortex that had experienced CSD. The slope of ERs increased after CSD relative to before CSD (124.7 ± 3.4 vs. 84.3 ± 2.4%; $P = 0.011$; Newman–Keuls test after significance in ANOVA, $F_{2,14} = 6.65$, $P = 0.009$; Fig. 4*C*), and the amplitude of ERs showed a similar increase (126.2 ± 4.1 vs. 81.3 ± 3.2; $P = 0.012$; Newman–Keuls test after significance in ANOVA, $F_{2,14} = 6.09$, $P = 0.012$; Fig. 4*D*). After recovery, both slope and amplitude of ERs were significantly different from the values immediately after CSD (slope, $P = 0.013$; amplitude, $P = 0.024$; Newman–Keuls test) but not significantly different from the baseline values (just before CSD). Moreover, the mean relative SWA occurring between the second and third ER sessions was positively correlated with the percentage of decrease in ER

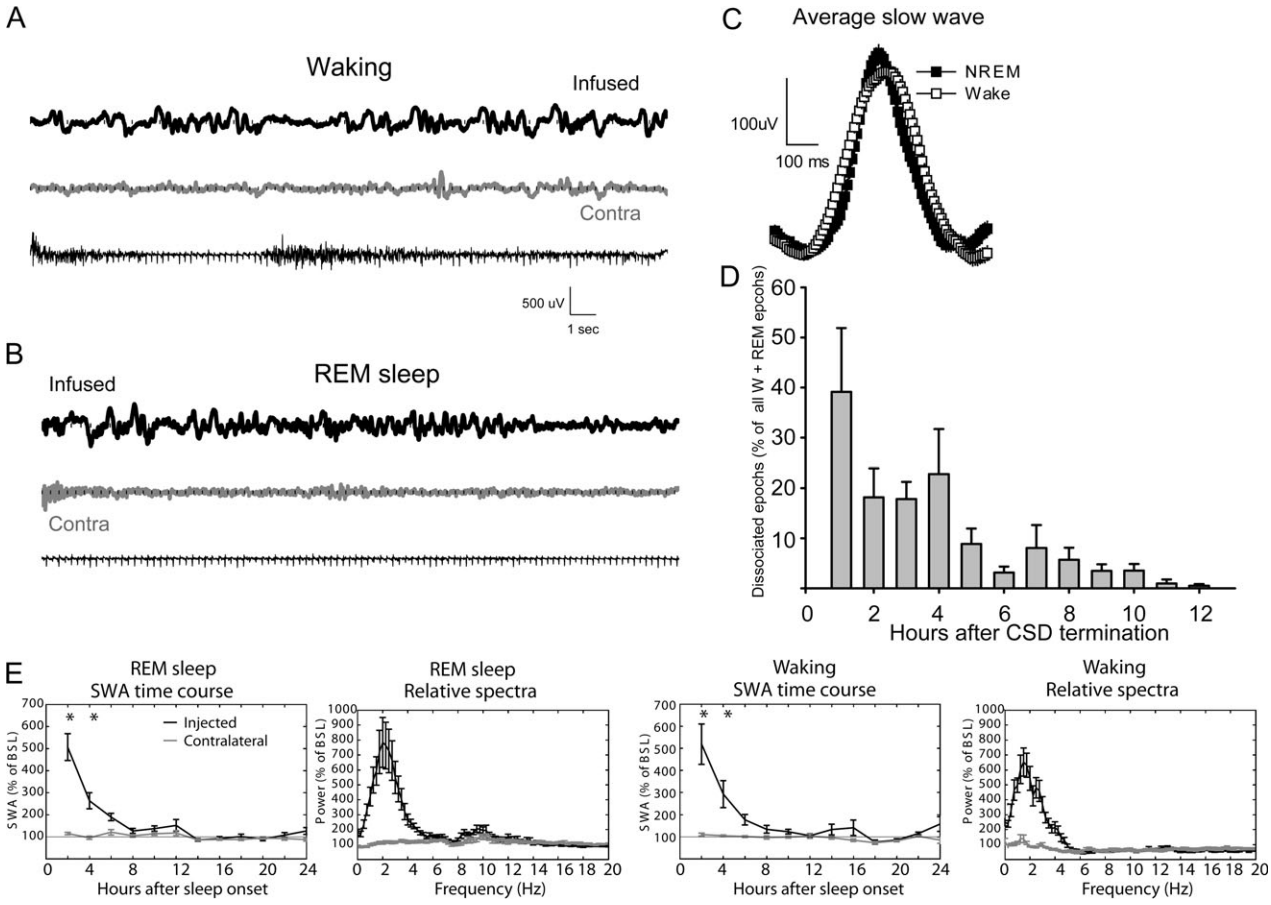

Figure 2. (*A*) Waking LFP raw data recordings (24 s). The top tracing was recorded approximately 30 min after the termination of CSD from the parietal derivation at the infused hemisphere. Bottom tracings: LFP from the contralateral parietal derivation and the nuchal EMG, respectively. (*B*) Recordings during REM sleep performed approximately 30 min after the termination of CSD from the previously infused hemisphere (top), the contralateral cortex (middle), and EMG. (*C*) Average slow wave recorded from the same derivation during waking post-CSD and during baseline NREM sleep ($n = 1$ rat, 287 waves/vigilance state contributed to the analysis). (*D*) Percentage of "dissociated" 4-s epochs of waking and REM sleep ($n = 6$; percentage for 1-h intervals over the first 12 h after the end of CSD). (*E*) Time course of SWA (expressed as percentage of 24-h baseline) and relative EEG power spectra (first 2 h after sleep onset) during REM sleep (left panels) and waking (right panels) in the affected hemisphere. $^*P < 0.01$ (Bonferroni correction after 2-way ANOVA).

slope (Pearson correlation coefficient; $r = 0.8047$, $P = 0.0291$) between the same sessions (Supplementary Fig. 3); in other words, the larger and more frequent were the NREM slow waves during the recovery period, the bigger was the decrease in corticocortical ERs.

In a subset of the same animals ($n = 4$), the stimulation site was reversed so that ERs were recorded from the nonaffected hemisphere. No difference was observed across the 3 recording sessions in either slope (Fig. 4*E*) or amplitude (Fig. 4*F*).

Immediate Early Gene Induction Occurs after CSD

To test whether the immediate early genes *Arc*, *BDNF*, and *NGFI-A* were induced by CSD, the entire right and left cortices were collected separately in 2 different sets of animals (not used for SWA analysis) that underwent either approximately 1 h or approximately 5 min of CSD. Messenger RNA levels in the affected and nonaffected hemispheres were measured by qPCR. After approximately 1-h CSD, all genes showed higher induction in the affected hemisphere relative to the contralateral one (affected vs. contralateral, percentage of the mean between the 2 hemispheres, *Arc* = 166.3 + 13.5 vs. 33.7 + 13.5; $P = 0.0125$; *NGFI-A* = 153.7 + 17.7 vs. 46.3 + 17.7; $P = 0.0686$; *BDNF* = 146.6 + 13.2 vs. 53.4 + 13.3; $P = 0.0391$; $n = 4$ rats, mean + SEM). Similar but smaller differential increases were also observed after approximately 5-min CSD (*Arc* = 157.2 + 15.6 vs. 42.8 + 15.6; $P = 0.0161$; *NGFI-A* = 114.0 + 3.4 vs. 86.0 + 3.4; $P = 0.0564$; *BDNF* = 128.0 + 10.2 vs. 72.0 + 10.2; $P = 0.0520$; $n = 7$ rats, mean + SEM).

Discussion

We found that immediately after CSD, corticocortical ERs recorded from the affected hemisphere (but not from the other side) have steeper slope and greater amplitude. It is well established that the strength of population excitatory postsynaptic currents is reflected by the slope of LFPs evoked by electrical stimuli (Rall 1967), and while LTP-inducing paradigms in vivo increase LFP slope (Bliss and Lomo 1973; Glazewski et al. 1998), long term depression paradigms reduce it (e.g., Fox et al. 2006). Thus, these results are consistent with the occurrence of synaptic potentiation in vivo as a result of CSD and are in line with previous in vitro studies in both rodent and human cortices (Footitt and Newberry 1998; Berger et al. 2008). But how could CSD, that is, spreading electrical silence, lead to synaptic potentiation? The precise mechanism remains unclear, but it is worth mentioning that each CSD cycle is preceded by a brief intense burst of single-unit activity (Grafstein 1956; Morlock et al. 1964; Sugaya et al. 1975), and

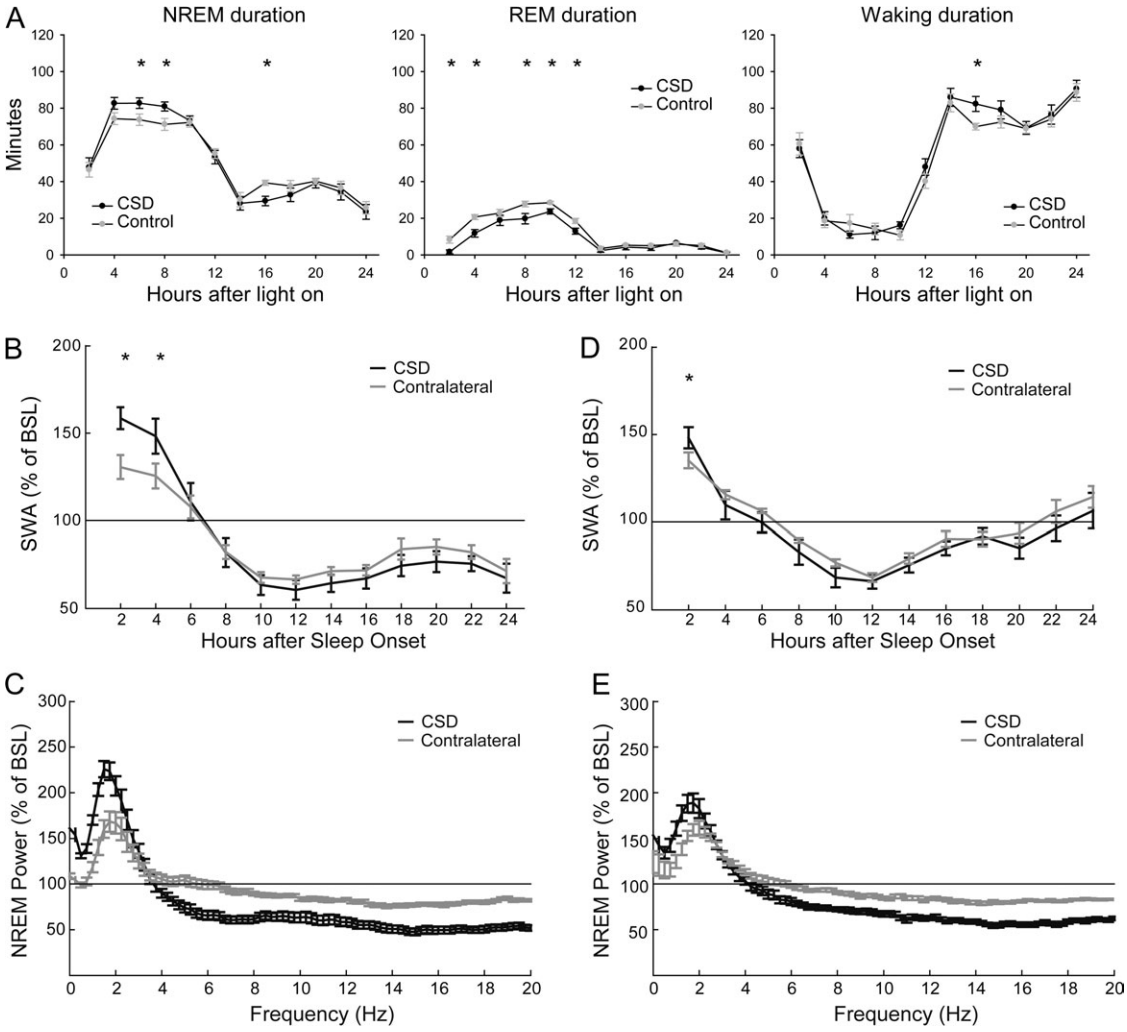

Figure 3. (*A*) Effects of CSD on the duration of sleep and waking expressed in 2-h intervals (control = after NaCl injection). (*B*, *D*) Changes in NREM SWA (0.5–4 Hz) after approximately 1-h (*B*) and 5-min (*D*) CSD ($n = 6$ for both groups). All data are normalized to the 24-h undisturbed baseline (BSL); $^*P < 0.01$ (Bonferroni correction after 2-way ANOVA). (*C*, *E*) EEG relative power spectra during recovery (0.25–20 Hz; mean of all NREM epochs occurring in the first 2 h of recovery) after approximately 1-h (*C*) and 5-min (*E*) CSD.

brief epileptic seizures are among the most powerful and best established paradigms for the induction of synaptic potentiation (Ben-Ari and Represa 1990; Reid and Stewart 1997). We tried to determine whether the amount of spiking activity during the hour of CSD could predict the change in ERs and/or in the following sleep SWA. However, in most rats, it was not possible to score the different phases of CSD for the entire hour because EEG artifacts prevented the quantification of spiking activity during periods of active waking.

We found that the expression of *Arc*, *BDNF*, and *NGFI-A* is increased after CSD, in agreement with previous reports (Kawahara et al. 1997; Kury et al. 2004; Urbach et al. 2006). Interestingly, after cortical brain ischemia, the same genes are upregulated in ipsilateral remote nonischemic cortex but not at the lesion site (Kokaia et al. 1995; Kury et al. 2004), suggesting that their induction can only occur in brain areas that did not undergo irreversible damage. *BDNF* is believed to confer ischemic tolerance through mechanisms independent from lesion effects (Kawahara et al. 1997), and it has been proposed that the induction of *BDNF* and other genes after CSD might promote tissue remodeling and cortical plasticity and confer tolerance toward subsequent ischemia (Urbach et al. 2006). *Arc*, *BDNF*, and *NGFI-A* have also been linked in vivo to synaptic plasticity and, in the case of *BDNF*, directly to synaptic potentiation (Davis et al. 2003; Bramham and Messaoudi 2005). Thus, their induction after CSD may reflect the occurrence of a protective cellular response, as well as the occurrence of synaptic potentiation, as also suggested by our in vivo ER data.

We also found that the recovery period after CSD is characterized by 2 kinds of phenomena, which may reflect the same or different underlying mechanisms. On one hand, we observed the appearance of large slow waves that were indistinguishable from those normally present during NREM sleep but occurred during quiet waking or when the rats were slowly moving around and during REM sleep. These waves were not continuous since even immediately after CSD they were present in less than half of all epochs of waking and REM sleep (as scored based on the contralateral hemisphere) and disappeared completely within 8–10 h. Most importantly, even in the first hours after CSD, they disappeared when the rat was actively exploring. On the other hand, after CSD, SWA during NREM sleep increased in the hemisphere that underwent CSD relative to the contralateral one. This asymmetry in NREM sleep SWA was no longer visible approximately 5 h after the end of

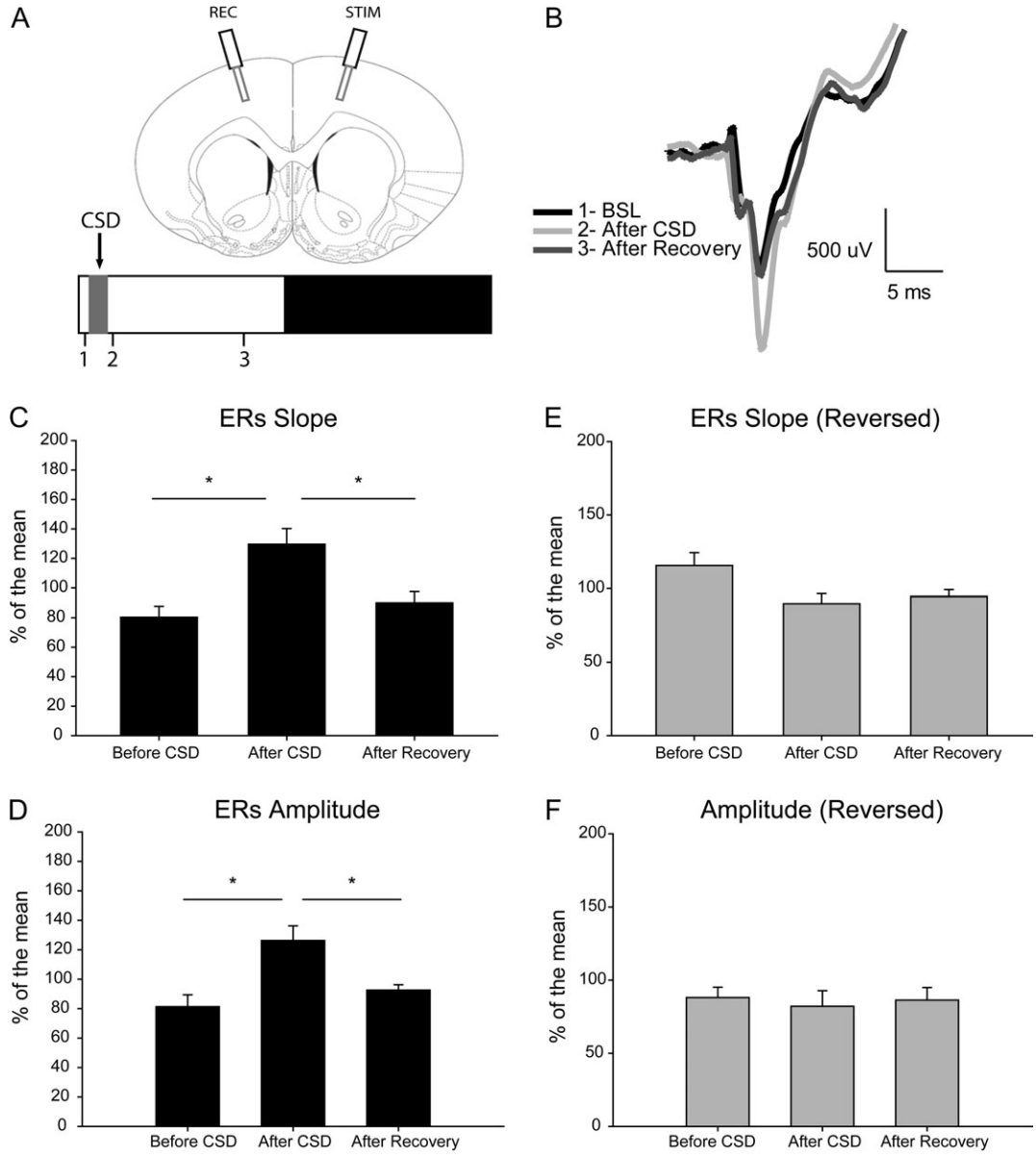

Figure 4. (*A*) Top: placement of LFP electrodes and example of the early component of ERs. Bottom: experimental design with 3 ERs recording sessions: 1, before CSD; 2, after CSD; and 3, after at least 4 h of recovery. (*B*) Representative average ERs from an individual animal for the 3 recording sessions. (*C*, *D*) Changes in ERs slope and amplitude ($n = 8$ rats, $^*P < 0.05$, Newman–Keuls test after ANOVA). (*E*, *F*) Lack of changes in slope and amplitude when ERs were recorded from the contralateral hemisphere ($n = 4$ rats). All data are expressed as percentage of the mean response (=100%) across the 3 recording sessions. BSL, baseline; REC, recording electrode; STIM, stimulation electrode.

CSD when most slow waves in waking and REM sleep had also disappeared. Thus, it is possible that the slow waves in waking and REM sleep and the SWA asymmetry during NREM sleep result from the same event triggered by CSD, perhaps of nonphysiological origin. For instance, CSD induces cell swelling, which in turn is associated with the activation of leakage potassium channels belonging to the 2-pore domain family (Kim 2003). A putative leakage potassium conductance is also thought to mediate the sleep slow oscillation (Steriade et al. 1993), the fundamental cellular phenomenon that underlies the occurrence of the slow waves as detected by the EEG. Thus, the activation of leakage channels may have triggered pathological slow waves in all behavioral states for several hours after CSD.

Another possibility is that slow waves were caused by a local disruption of cholinergic transmission in the cerebral cortex. Cholinergic antagonists such as atropine induce cortical slow waves in all behavioral states (Bradley et al. 1968), and CSD virtually silences neuronal activity within the basal forebrain, where many cholinergic neurons are located (Szentgyorgyi et al. 2006). Moreover, slow waves induced by cholinergic antagonists subside during active waking (Buzsaki et al. 1988) similar to the disappearance of slow waves with active exploration in our rats. Yet, the basal forebrain contains also many noncholinergic (most likely glutamatergic) neurons whose lesion may affect EEG activation (Allen et al. 2006; Gritti et al. 2006; Kaur et al. 2008). Thus, it is likely that more than one neurotransmitter/neuromodulator is affected by CSD.

Other underlying mechanisms for both phenomena are also possible and not mutually exclusive and may also explain why CSD was followed by an increase in NREM sleep. CSD induces the expression of proinflammatory genes that have been involved in NREM sleep regulation, namely *TNF alpha* and *IL-1 beta* (Jander et al. 2001; Krueger et al. 2008). Moreover, CSD upregulates the expression of neuronal *COX-2*, and a previous study has suggested that *COX-2* may mediate the post-CSD increase in NREM sleep duration through the production of prostaglandins (Cui et al. 2008). Finally, during CSD, ATP (Lauritzen et al. 1990), pH (Csiba et al. 1985), and glucose (Csiba et al. 1985; Lauritzen et al. 1990) decrease, while lactate production (Hashemi et al. 2009), cAMP (Krivanek 1976), and ADP (Lauritzen et al. 1990) increase. These findings suggest that CSD is associated with energy depletion, and indeed, a recent in vivo study using NADH fluorescence 2-photon imaging found that CSD is caused by a transient increase in oxygen demands exceeding vascular supplies (Takano et al. 2007). Interestingly, energy depletion in localized brain areas, at least in the basal forebrain, can also increase the duration of NREM sleep without affecting REM sleep (Kalinchuk et al. 2003). However, the fact that the waking slow waves in our rats could be suppressed by active exploration makes energy depletion an unlikely explanation for their occurrence.

It cannot be excluded that the asymmetry in sleep SWA "coexists" with the presence of slow waves during waking and REM sleep. The NREM SWA increase may have a different more physiological origin related to the synaptic potentiation triggered by CSD, as suggested by the changes in cortical ERs and the induction of *BDNF*. There is increasing experimental evidence showing that SWA changes reflect changes in synaptic strength, and recent evidence suggests a link between the occurrence of synaptic potentiation during waking and subsequent sleep need. Specifically in rats, waking exploratory behavior, cortical expression of *BDNF*, and SWA are positively correlated (Huber et al. 2007), and increasing active waking by local infusion of NMDA into the basal forebrain produces a subsequent increase in SWA (Wigren et al. 2007). In rats, local cortical application of *BDNF*, a molecule causally linked to LTP, also produces a localized increase in SWA (Faraguna et al. 2008), while decreasing TNF alpha expression, whose release increases surface AMPA expression, causes a reduction in SWA (Taishi et al. 2007). Training on a reaching task known to induce LTP also results in a local increase in SWA in the activated rat motor region (Hanlon et al. 2009). Consistent with these animal studies, in humans, cortical potentiation and depression triggered by paired associative stimulation result in increased and decreased SWA, respectively (Huber et al. 2008).

In summary, although energy depletion after CSD and other nonphysiological phenomena may explain the occurrence of slow waves in waking and REM sleep as well as the increase in SWA during NREM sleep, the latter may also result, at least in part, from the increase in synaptic strength triggered by CSD. Independent of the underlying mechanisms, these results show that CSD, which is thought to be involved in the pathogenesis of migraine, triggers in vivo profound effects on the waking and sleep EEG that last for several hours.

Funding

National Institute of Mental Health (P20 MH077967 to C.C.); National Institutes of Health director's Pioneer award (to G.T.).

Supplementary Material

Supplementary material can be found at: http://www.cercor.oxfordjournals.org/

Notes

Conflict of Interest: None declared.

References

Achermann P, Borbely AA. 2003. Mathematical models of sleep regulation. Front Biosci. 8:s683–s693.

Allen TG, Abogadie FC, Brown DA. 2006. Simultaneous release of glutamate and acetylcholine from single magnocellular "cholinergic" basal forebrain neurons. J Neurosci. 26:1588–1595.

Ben-Ari Y, Represa A. 1990. Brief seizure episodes induce long-term potentiation and mossy fibre sprouting in the hippocampus. Trends Neurosci. 13:312–318.

Berger M, Speckmann EJ, Pape HC, Gorji A. 2008. Spreading depression enhances human neocortical excitability in vitro. Cephalalgia. 28:558–562.

Best PJ, Orr J, Pointer JE. 1975. Differential effects of cortical ablation and spreading depression on sensitivity to footshock: implications for the role of the cortex in learning. Physiol Behav. 14:801–807.

Bliss TV, Lomo T. 1973. Long-lasting potentiation of synaptic transmission in the dentate area of the anaesthetized rabbit following stimulation of the perforant path. J Physiol. 232:331–356.

Bradley PB, Fink M. Collegium Internationale Neuro-psychopharmacologicum. Congress 1968. Anticholinergic drugs and brain functions in animals and man. Amsterdam: Elsevier Pub. Co.

Bramham CR, Messaoudi E. 2005. BDNF function in adult synaptic plasticity: the synaptic consolidation hypothesis. Prog Neurobiol. 76:99–125.

Buzsaki G, Bickford RG, Ponomareff G, Thal LJ, Mandel R, Gage FH. 1988. Nucleus basalis and thalamic control of neocortical activity in the freely moving rat. J Neurosci. 8:4007–4026.

Cirelli C, Gutierrez CM, Tononi G. 2004. Extensive and divergent effects of sleep and wakefulness on brain gene expression. Neuron. 41:35–43.

Csiba L, Paschen W, Mies G. 1985. Regional changes in tissue pH and glucose content during cortical spreading depression in rat brain. Brain Res. 336:167–170.

Cui Y, Kataoka Y, Inui T, Mochizuki T, Onoe H, Matsumura K, Urade Y, Yamada H, Watanabe Y. 2008. Up-regulated neuronal COX-2 expression after cortical spreading depression is involved in non-REM sleep induction in rats. J Neurosci Res. 86:929–936.

Davis S, Bozon B, Laroche S. 2003. How necessary is the activation of the immediate early gene zif268 in synaptic plasticity and learning? Behav Brain Res. 142:17–30.

Faraguna U, Vyazovskiy VV, Nelson AB, Tononi G, Cirelli C. 2008. A causal role for brain-derived neurotrophic factor in the homeostatic regulation of sleep. J Neurosci. 28:4088–4095.

Footitt DR, Newberry NR. 1998. Cortical spreading depression induces an LTP-like effect in rat neocortex in vitro. Brain Res. 781:339–342.

Fox CJ, Russell KI, Wang YT, Christie BR. 2006. Contribution of NR2A and NR2B NMDA subunits to bidirectional synaptic plasticity in the hippocampus in vivo. Hippocampus. 16:907–915.

Glazewski S, Herman C, McKenna M, Chapman PF, Fox K. 1998. Long-term potentiation in vivo in layers II/III of rat barrel cortex. Neuropharmacology. 37:581–592.

Grafstein B. 1956. Mechanism of spreading cortical depression. J Neurophysiol. 19:154–171.

Gritti I, Henny P, Galloni F, Mainville L, Mariotti M, Jones BE. 2006. Stereological estimates of the basal forebrain cell population in the rat, including neurons containing choline acetyltransferase, glutamic acid decarboxylase or phosphate-activated glutaminase and colocalizing vesicular glutamate transporters. Neuroscience. 143:1051–1064.

Hanlon EC, Faraguna U, Vyazovskiy VV, Tononi G, Cirelli C. 2009. Effects of skilled training on sleep slow wave activity and cortical gene expression in the rat. Sleep. 32:719–729.

Hashemi P, Bhatia R, Nakamura H, Dreier JP, Graf R, Strong AJ, Boutelle MG. 2009. Persisting depletion of brain glucose following cortical spreading depression, despite apparent hyperaemia: evidence for risk of an adverse effect of Leao's spreading depression. J Cereb Blood Flow Metab. 29:166–175.

Huber R, Maatta S, Esser SK, Sarasso S, Ferrarelli F, Watson A, Ferreri F, Peterson MJ, Tononi G. 2008. Measures of cortical plasticity after transcranial paired associative stimulation predict changes in electroencephalogram slow-wave activity during subsequent sleep. J Neurosci. 28:7911–7918.

Huber R, Tononi G, Cirelli C. 2007. Exploratory behavior, cortical BDNF expression, and sleep homeostasis. Sleep. 30:129–139.

Jander S, Schroeter M, Peters O, Witte OW, Stoll G. 2001. Cortical spreading depression induces proinflammatory cytokine gene expression in the rat brain. J Cereb Blood Flow Metab. 21:218–225.

Kalinchuk AV, Urrila AS, Alanko L, Heiskanen S, Wigren HK, Suomela M, Stenberg D, Porkka-Heiskanen T. 2003. Local energy depletion in the basal forebrain increases sleep. Eur J Neurosci. 17:863–869.

Kaur S, Junek A, Black MA, Semba K. 2008. Effects of ibotenate and 192IgG-saporin lesions of the nucleus basalis magnocellularis/substantia innominata on spontaneous sleep and wake states and on recovery sleep after sleep deprivation in rats. J Neurosci. 28:491–504.

Kawahara N, Croll SD, Wiegand SJ, Klatzo I. 1997. Cortical spreading depression induces long-term alterations of BDNF levels in cortex and hippocampus distinct from lesion effects: implications for ischemic tolerance. Neurosci Res. 29:37–47.

Kim D. 2003. Fatty acid-sensitive two-pore domain K+ channels. Trends Pharmacol Sci. 24:648–654.

Kitahara Y, Taga K, Abe H, Shimoji K. 2001. The effects of anesthetics on cortical spreading depression elicitation and c-fos expression in rats. J Neurosurg Anesthesiol. 13:26–32.

Kokaia Z, Zhao Q, Kokaia M, Elmer E, Metsis M, Smith ML, Siesjo BK, Lindvall O. 1995. Regulation of brain-derived neurotrophic factor gene expression after transient middle cerebral artery occlusion with and without brain damage. Exp Neurol. 136:73–88.

Krivanek J. 1976. Adenosine 3′,5′-monophosphate in rat cerebral cortex: effect of potassium ions in vivo (cortical spreading depression). J Neurochem. 26:413–415.

Krueger JM, Obal F Jr. Kapas L, Fang J. 1995. Brain organization and sleep function. Behav Brain Res. 69:177–185.

Krueger JM, Rector DM, Roy S, Van Dongen HP, Belenky G, Panksepp J. 2008. Sleep as a fundamental property of neuronal assemblies. Nat Rev Neurosci. 9:910–919.

Kury P, Schroeter M, Jander S. 2004. Transcriptional response to circumscribed cortical brain ischemia: spatiotemporal patterns in ischemic vs. remote non-ischemic cortex. Eur J Neurosci. 19:1708–1720.

Lauritzen M. 1994. Pathophysiology of the migraine aura. The spreading depression theory. Brain. 117(Pt 1):199–210.

Lauritzen M, Hansen AJ, Kronborg D, Wieloch T. 1990. Cortical spreading depression is associated with arachidonic acid accumulation and preservation of energy charge. J Cereb Blood Flow Metab. 10:115–122.

Leao AA. 1944. Spreading depression of activity in the cerebral cortex. J Neurophysiol. 7:359–390.

Monda M, Viggiano A, De Luca V. 2000. Functional decortication lowers ventromedial hypothalamic activation induced by hippocampal neostigmine injection. Cereb Cortex. 10:1242–1246.

Morlock NL, Mori K, Ward AA Jr. 1964. A study of single cortical neurons during spreading depression. J Neurophysiol. 27:1192–1198.

Nedergaard M, Hansen AJ. 1988. Spreading depression is not associated with neuronal injury in the normal brain. Brain Res. 449:395–398.

Rall W. 1967. Distinguishing theoretical synaptic potentials computed for different soma-dendritic distributions of synaptic input. J Neurophysiol. 30:1138–1168.

Reid IC, Stewart CA. 1997. Seizures, memory and synaptic plasticity. Seizure. 6:351–359.

Shibata M, Bures J. 1974. Functional decortication employing reverberating cortical spreading depression: experimental evaluation of advantages and limitations. Exp Neurol. 45:415–423.

Smith JM, Bradley DP, James MF, Huang CL. 2006. Physiological studies of cortical spreading depression. Biol Rev Camb Philos Soc. 81:457–481.

Steriade M, Nunez A, Amzica F. 1993. A novel slow (< 1 Hz) oscillation of neocortical neurons in vivo: depolarizing and hyperpolarizing components. J Neurosci. 13:3252–3265.

Sugaya E, Takato M, Noda Y. 1975. Neuronal and glial activity during spreading depression in cerebral cortex of cat. J Neurophysiol. 38:822–841.

Szentgyorgyi V, Balatoni B, Toth A, Detari L. 2006. Effect of cortical spreading depression on basal forebrain neurons. Exp Brain Res. 169:261–265.

Taishi P, Churchill L, Wang M, Kay D, Davis CJ, Guan X, De A, Yasuda T, Liao F, Krueger JM. 2007. TNFalpha siRNA reduces brain TNF and EEG delta wave activity in rats. Brain Res. 1156:125–132.

Takano T, Tian GF, Peng W, Lou N, Lovatt D, Hansen AJ, Kasischke KA, Nedergaard M. 2007. Cortical spreading depression causes and coincides with tissue hypoxia. Nat Neurosci. 10:754–762.

Tobler I, editor. 2005. Phylogeny of sleep regulation. 4th ed. Philadelphia (PA): Elsevier Saunders.

Tononi G, Cirelli C. 2003. Sleep and synaptic homeostasis: a hypothesis. Brain Res Bull. 62:143–150.

Tononi G, Cirelli C. 2006. Sleep function and synaptic homeostasis. Sleep Med Rev. 10:49–62.

Urbach A, Bruehl C, Witte OW. 2006. Microarray-based long-term detection of genes differentially expressed after cortical spreading depression. Eur J Neurosci. 24:841–856.

Vyazovskiy VV, Cirelli C, Pfister-Genskow M, Faraguna U, Tononi G. 2008. Molecular and electrophysiological evidence for net synaptic potentiation in wake and depression in sleep. Nat Neurosci. 11:200–208.

Walz W. 2000. Role of astrocytes in the clearance of excess extracellular potassium. Neurochem Int. 36:291–300.

Wigren HK, Schepens M, Matto V, Stenberg D, Porkka-Heiskanen T. 2007. Glutamatergic stimulation of the basal forebrain elevates extracellular adenosine and increases the subsequent sleep. Neuroscience. 147:811–823.